PAPER • OPEN ACCESS

The effect of microstructure on the dynamic mechanical properties of carbon fiber and carbon nanotube reinforced multi-scale composites with a polyamide 6 matrix

To cite this article: R Petrény and L Mészáros 2020 *IOP Conf. Ser.: Mater. Sci. Eng.* **903** 012021

View the article online for updates and enhancements.

The effect of microstructure on the dynamic mechanical properties of carbon fiber and carbon nanotube reinforced multi-scale composites with a polyamide 6 matrix

R Petrény[1] and L Mészáros[1, 2]

[1]Department of Polymer Engineering, Faculty of Mechanical Engineering, Budapest University of Technology and Economics, Budapest, Hungary
[2]MTA–BME Research Group for Composite Science and Technology, Budapest, Hungary

E-mail: meszaros@pt.bme.hu

Abstract. We investigated the microstructure and the related dynamic mechanical properties of carbon fiber and carbon nanotube (CNT) reinforced, polyamide 6 (PA6) matrix multi-scale composites. Differential scanning calorimetry (DSC) showed that in composites reinforced with only carbon nanotubes, the aggregated nanotubes have a moderate crystal nucleating effect. However, in the hybrids, the carbon fibers and the uniformly dispersed CNTs have a notable crystal nucleating effect. It means that a crystalline interphase is formed around both the carbon fibers and the carbon nanotubes. As the interphase has higher modulus than the bulk matrix, it has an additional reinforcing effect and transfers the load better to the microfibers. We confirmed this theory by dynamic mechanical analysis.

1. Introduction

The development of multi-scale composites with a thermoplastic polymer matrix is one of the most popular research areas today. However, the widespread use of these materials in practice is limited by the fact that their strength and their dynamic mechanical properties often differ from what is expected from conventional fiber-reinforced composites. This is because nanostructured composites have a different microstructure than conventional fiber-reinforced composites, which may result in different reinforcing mechanisms [1, 2].

Currently, the designing of nanocomposites is based on conventional composite mechanics, which ignores these differences in material structure, thus providing an inaccurate estimate of the macroscopic mechanical properties of nanocomposites. Since the structural and mechanical properties of nanocomposites are poorly understood, designing them accurately is a great challenge and so their use in industrial practice remains modest [3, 4].

In composites, as a result of interfacial interactions between the matrix and reinforcement interface, a three-dimensional interphase layer is formed, whose properties are different from those of the matrix and reinforcing material itself. As nanoparticles have a large surface/volume ratio, the matrix-nanoparticle interface is large, thus the volume ratio of this interphase layer is significant in nano- and hybrid composites, and moreover, it influences the mechanical behavior of the composite. Therefore, accurate designing of such composites requires precise knowledge of the characteristics of this interphase [5-8].

There is a more and more widely accepted approach that, in semi-crystalline thermoplastic polymers, three different phases can be distinguished: a crystalline fraction, a rigid amorphous fraction and mobile amorphous fractions that surround them. Several publications reported that nano-sized and micro-sized reinforcing materials can have a crystal nucleating effect in a thermoplastic polymer matrix, so the interphase around the reinforcement should be mostly crystalline. However, due to the interactions between the matrix and the reinforcement, the movement of the polymer chains is hampered around the reinforcement, which hinders crystallization and results in a rigid amorphous interphase. Moreover, around the crystallites, a similar rigid amorphous interphase is formed. As the rigid amorphous phase needs more energy for segmental movement, the heat capacity step at the glass transition is lower if the rigid amorphous fraction is larger. This means that the volume fractions of the rigid and the mobile amorphous parts are calculable. The structure of the above-mentioned three phases can be analyzed by differential scanning calorimetry, as they have different thermal characteristics [8, 9].

Recently many publications deal with the microstructure of the interphases; however, the effect of the interphase structure on the mechanical properties is less investigated. If a crystalline or a rigid amorphous interphase surrounds the reinforcing material, the mobility of the polymer molecules is lower in either of them, compared to the bulk matrix. This immobilized interphase layer helps transfer the stress from the matrix to the reinforcement. Macroscopically, it results in a higher modulus and lower dynamic dampening, which can be detected by dynamic mechanical analysis [9-14].

The aim of this research was to analyze the microstructure, and particularly, the interphases of carbon fiber and carbon nanotube reinforced multi-scale composites and investigate the effect of the microstructure on mechanical properties.

2. Materials and methods

We used polyamide 6 (PA6) homopolymer (SHULAMID 6 MV 13 F) manufactured by A. Schulman GmbH as matrix material for the composites. It had a density of 1.13 g/cm^3 (at room temperature) and a melt flow index of 14.7 g/10 min (2.16 kg, 230 °C). The multi-wall carbon nanotubes used as reinforcing material were produced by Nanocyl s.a. The NANOCYL NC7000 carbon nanotube (CNT) had an average diameter of 9.5 nm and a length of 1.5 μm. As fiber reinforcement, we used Panex 35 Chopped Pellet 95 type carbon fiber (CF) manufactured by Zoltek Zrt. The fibers had a mean initial length of 6 mm and a diameter of 8.3 μm. The density of the fibers was 1.81 g/cm^3.

The PA6 granules were dried for 4 hours at 80 °C, after which the nanotubes and carbon fibers were mixed first by mechanical mixing in a closed vessel and then with a Labtech LTE 26-44 twin screw extruder. The zone temperatures were 230 °C, 230 °C, 235 °C, 235 °C, 240 °C and 240 °C towards the die, and screw rotational speed was 25 rpm. After granulation and re-drying for 4 hours at 80 °C, MSZ EN ISO 527-2-1A type specimens were produced with an Arburg Allrounder 370 S 700-290 injection molding machine.

We made PA6 matrix nanocomposites with 0, 0.25, 0.5, 0.75 and 1 wt% carbon nanotube content (PA6, PA6+0.25CNT, PA6+0.5CNT, PA6+0.75CNT, PA6+1CNT), and composites reinforced with 30 wt% carbon fiber, and 0, 0.25, 0.5, 0.75 and 1 wt% carbon nanotube content (PA6+30CF, PA6+30CF +0.25CNT, PA6+30CF +0.5CNT, PA6+30CF +0.75CNT, PA6+30CF +1CNT).

For morphological tests, we used a TA Instruments Q2000 type DSC in modulated DSC (MDSC) mode. The test temperature range was 0-250 °C with a heating and cooling rate of 5 °C/min, the amplitude of modulation was 1 °C, and its period was 60 s. The mass of the test samples ranged from 10 to 15 mg. The volume ratio of rigid amorphous phase (ϕ_{RAF}) in the matrix is [9]:

$$\phi_{RAF} = 1 - \phi_{MAF} - \phi_C,$$

where ϕ_{MAF} is the volume ratio of the mobile amorphous fraction, and ϕ_C is the crystalline fraction. For this, the volume ratio of the mobile amorphous fraction is calculated as follows [9]:

$$\phi_{MAF} = \frac{\Delta C_p}{\Delta C_{p,0}},$$

where ΔC_p is the specific heat increment of the semi-crystalline polymer or composite, $\Delta C_{p,0}$ is the specific heat increment of the fully amorphous polymer in the glass transition temperature range. In the

case of polyamide 6, $\Delta C_{p,0} = 0,475 \frac{J}{g°C}$, according to the literature. Crystallinity can be calculated with the following equation [9]:

$$\phi_C = \frac{\Delta H}{\Delta H_0 (1 - \varphi_R)}$$

The related ΔH is the crystalline melting enthalpy as determined by the DSC test, $\Delta H_0 = 240$ J/g is the melting enthalpy of 100% crystalline polyamide 6, and φ_R is the weight ratio of the reinforcing material [9].

The fracture surfaces of the tensile tested specimens were investigated with a Jeol 6380 LA-type scanning electron microscope (SEM) after they were sputtered with gold.

Dynamic mechanical properties were measured with a TA Instruments Q800 dynamic mechanical analyzer (DMA) in 3-point bending mode. The temperature range was 0-210 °C with a heating speed of 3 °C/min. The amplitude of deformation excitation was 0.02% and the frequency was 1 Hz.

3. Results and discussion

3.1. The microstructure of the nano-and hybrid composites

In the composites reinforced with only carbon nanotubes, the crystalline fraction slightly increased with increasing carbon nanotube content, which indicates the crystal nucleating effect of the nanoparticles (Figure 1.a). The crystal nucleating effect of carbon nanotubes in the PA6 matrix was investigated in one of our former articles [10]. However, the rigid amorphous fraction showed a slight decrease with increasing carbon nanotube content. This can be attributed to the fact that the rigid amorphous fraction can be found in both the interphase around the crystalline fraction and the interphase around the nanoparticles, so the volume fraction of the rigid amorphous phase is significantly influenced by the size of the surface of the nanotubes and the crystallites . If the carbon nanotubes form large aggregates as it can be seen on the SEM images (Figure 1.b), the crystallites formed around them are larger, which results in a smaller surface/volume ratio of the crystallites and a smaller rigid amorphous fraction despite the higher crystallinity.
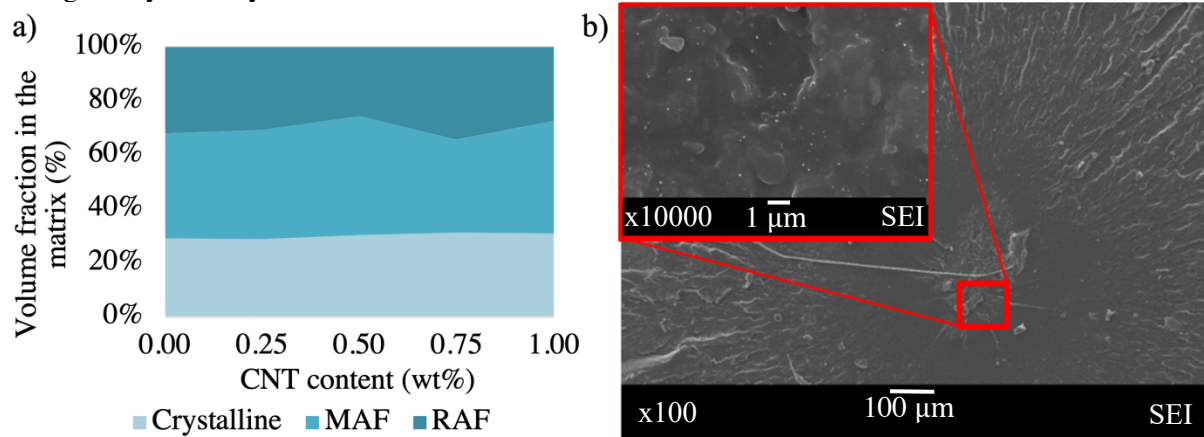
Figure 1. a) Volume fraction of the crystalline, the rigid amorphous (RAF) and the mobile amorphous (MAF) fractions in the matrix of the nanocomposites
b) SEM images of a CNT aggregate on the fracture surface of the PA+0.5CNT nanocomposite

To prove this theory, we investigated the cooling curves to understand the crystallization process in the nanocomposites. The crystallization peaks became wider as nanotube content increased, which was related to the size distribution of the crystallites, i.e. with higher nanotube content, the scatter of crystallite size increased (Figure 2). The crystallization peaks also shifted to higher temperatures with increasing nanotube content, which shows that the nanotubes had a crystal nucleation effect [11].
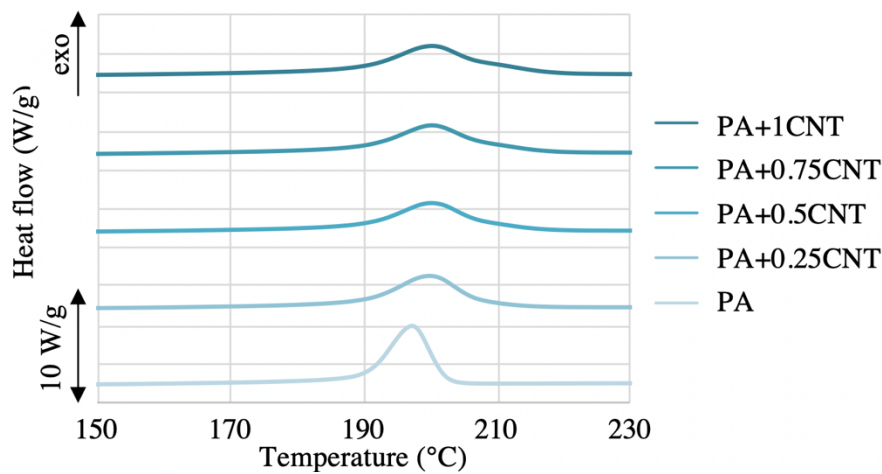
Figure 2. Cooling DSC curves of the nanocomposites

Table 1 shows that the width at half maximum of the peaks became wider with increasing carbon nanotube content, which clearly indicates the wider distribution of crystallite size [11]. The explanation for this is that during processing, the carbon nanotubes remained mainly in aggregated form, and the size distribution of these aggregates was wide [10]. As the starting points of crystal nucleation were these aggregates, the size distribution of the crystallites should also be wide. The crystallization peaks shifted to higher temperatures with increasing nanotube content, which proves the crystal nucleating effect of the nanotubes. The higher crystallization peak temperature means that in the nanocomposites, the crystallites became larger, which resulted in a smaller surface/volume ratio of the crystallites. This explains the smaller volume fraction of the surrounding rigid amorphous interphase.

Table 1. Peak temperature (T_p) and full width at half maximum of the peaks (T_{fwhm}) of the cooling curves of the nanocomposite

Sample	T_{fwhm}	T_p
	(°C)	(°C)
$PA6$	6.9	197.3
$PA6 + 0.25CNT$	10.7	199.9
$PA6 + 0.5CNT$	11.7	200.2
$PA6 + 0.75CNT$	12.0	200.2
$PA6 + 1CNT$	12.6	200.3

In the carbon fiber reinforced composites, the crystalline fraction slightly, and the rigid amorphous fraction significantly increased compared to the pure PA6; adding carbon nanotubes to fiber reinforced composites increased the volume fraction of the above-mentioned fractions even further (Figure 3.a). The increase in the rigid amorphous fraction can be related to both the increase of the crystalline fraction and the decrease of crystallite size. This effect may be explained by that the more uniformly dispersed carbon nanotubes influences the crystallization process differently, than the aggregated ones (Figure 3.b).
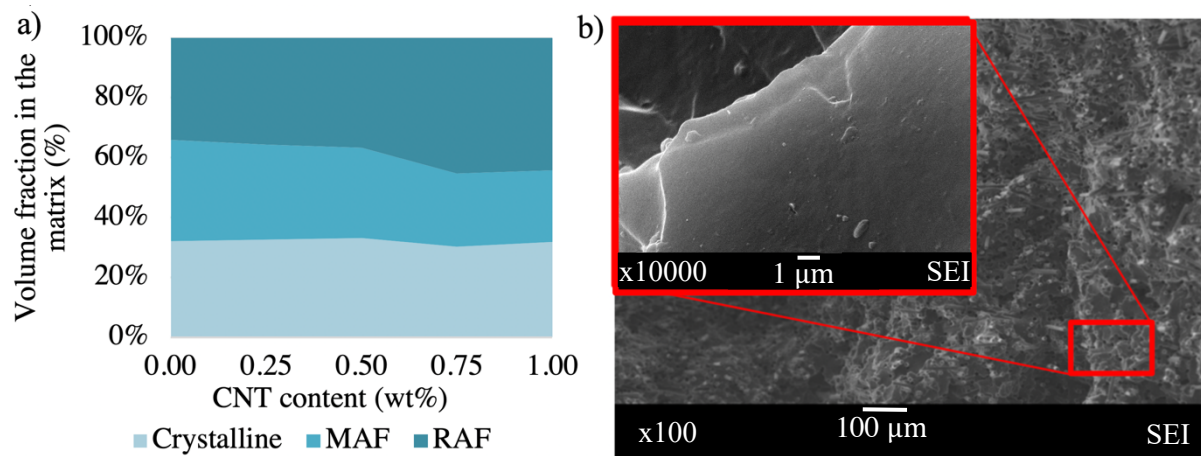
Figure 3. a) Volume fraction of the crystalline, the rigid amorphous (RAF) and the mobile amorphous (MAF) fractions in the matrix of the carbon fiber reinforced composites
b) SEM images of the fracture surface of the PA+30CF+0.5CNT nanocomposite. No aggregates visible, uniformly dispersed nanotubes (white spots) on the higher magnification image

When carbon fiber is added to polyamide 6, a moderate crystal nucleating effect can be observed, which did not significantly change the size and the size distribution of the crystallites compared to the pure PA6. However, crystallinity slightly increased. On the cooling curves of the hybrid composites, an additional peak can be observed around 210 °C, which became more significant with higher nanotube content (Figure 4).
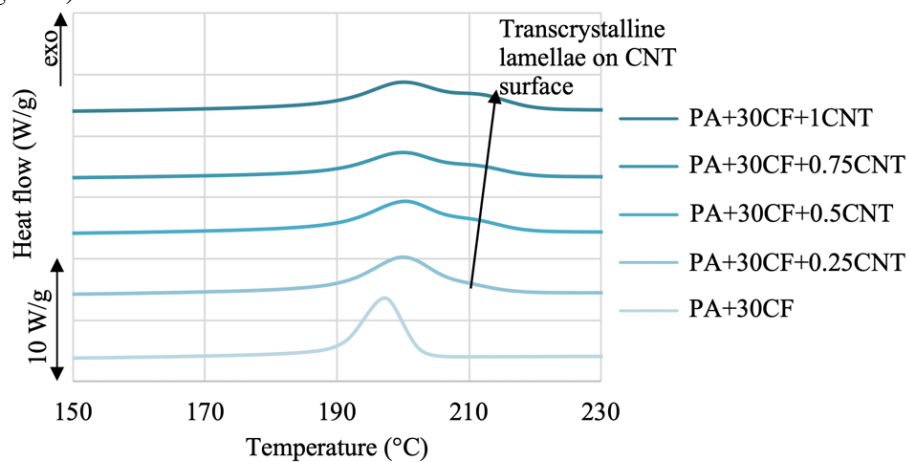
Figure 4. Cooling DSC curves of the composites containing carbon fiber

Brosse et al. [15] reported that the second crystallization peak in carbon nanotube reinforced PA6 indicates trans-crystalline lamellae that grow perpendicularly on the surface of the well dispersed nanotubes. In our hybrid composites, this second peak also appeared and became more significant and shifted towards higher temperatures with the increasing nanotube content which indicates that a significant amount of well dispersed nanotubes are present in the composite (Table 2). If these trans-crystalline lamellae grew on the surface of the dispersed nanotubes, crystallite size should be smaller than in the nanocomposites, where the crystals grew on large nanotube aggregates. Therefore, besides higher crystallinity, the smaller average crystallite size may be the explanation for the increase of the rigid amorphous phase in the hybrid composites.

Table 2. Peak temperatures (T_{p1} and T_{p2}) of crystallization of the composites containing carbon fiber

Sample	T_{p1} (°C)	T_{p2} (°C)
$PA6 + 30CF$	197.2	-
$PA6 + 30CF + 0.25CNT$	200.1	209.12
$PA6 + 30CF + 0.5CNT$	199.9	204.17
$PA6 + 30CF + 0.75CNT$	200.4	206.13
$PA6 + 30CF + 1CNT$	200.0	207.83

The DSC tests showed that in the nanocomposites, the carbon nanotubes had a moderate crystal nucleating effect. This means that the carbon nanotube aggregates were surrounded by a crystalline interphase, which was surrounded by a rigid amorphous interphase (Figure 5.a). Similarly, in the hybrid composites, both the carbon fibers and the well-dispersed carbon nanotubes were surrounded by a two-layer interphase; the inner layer was the crystalline and the outer one was the rigid amorphous phase (Figure 5.b).

a)

Rigid amorphous interphase¶

Crystalline interphase¶

CNT aggregate¶

b)

Carbon fiber¶

Crystalline interphase¶

CNT¶

Rigid amorphous interphase¶
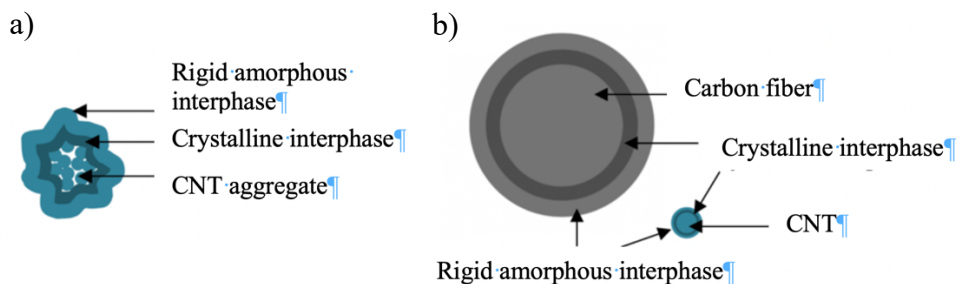
Figure 5. a) the interphase model of the nanocomposites,
b) the interphase model of the hybrid composites

3.2. Dynamic mechanical behavior of the nano- and hybrid composites

The effect of the two-layer interphase on the viscoelastic behavior was perceptible on the increase of the storage modulus (Figure 6.a), which indicates that the nanocomposites behaved more elastic compared to the pure PA6. This has an essential role in the case of the long-term mechanical properties, especially the creep resistance of the materials. The loss factor ($tan\delta$) curves (Figure 6.b) showed the changes in the mechanical properties more spectacularly, in the case of the nanocomposites, the first peak was typically lower than that of the pure PA6. This means that the magnitude of the drop in the storage modulus at the glass transition temperature was lower by adding nanotubes to the composite. The position of this first peak is shifted towards higher temperatures in the nanocomposites, which means that the drop in the storage modulus is not only lower compared to the pure PA6, but also the temperature is higher, where it happens. As this first peak shows the glass transition process, where the micro-Brown movements of the amorphous parts of the polymer chains start, it can be stated that this improvement of the mechanical properties is not only due to the nanotubes themselves, but the change in the microstructure of the matrix. This may be explained by that even the aggregated carbon nanotubes effectively blocked the movement of the polymer chain segments, which hampered the glass transition process. However, in the carbon nanotube filled PA6, there was no clear correlation between the position of the glass transition peak and nanotube content, due to the stochastic size and size distribution of the nanotube aggregates.

a)   b)
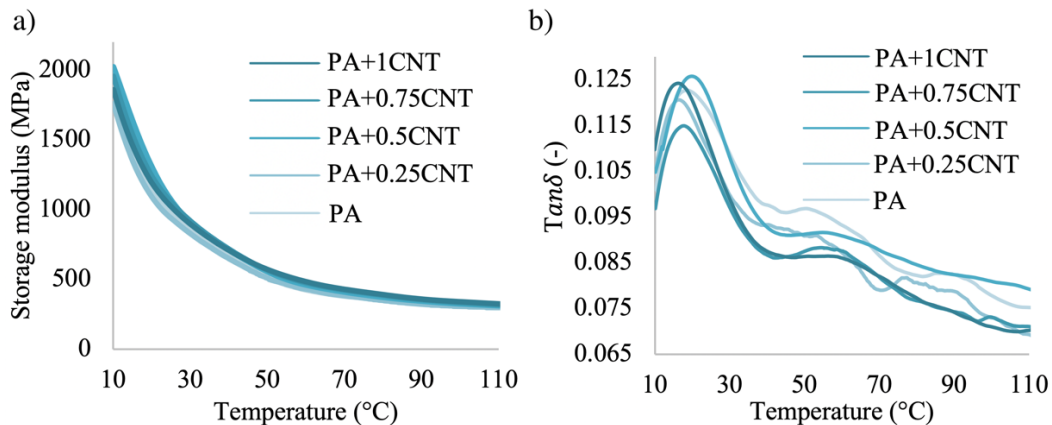
Figure 6. a) Storage modulus and b) loss factor curves of the nanocomposites

Besides the previously mentioned glass transition peak, an additional peak can be observed between 40 and 60 °C, which indicates the drop in the storage modulus caused by the segment motions in the rigid amorphous fractions, i.e. the outer layer of the interphase. By adding carbon nanotubes to the PA6, this peak slightly decreased, which indicates that the drop in the storage modulus slightly decreased by the presence of this rigid amorphous interphase layer. The size and the position of this peak does not show any correlation with the nanotube content, which is in good agreement with the relationship between the nanotube content and the volume fraction of the rigid amorphous interphase.

In the case of the composites containing carbon fibers, the composite reinforced with only carbon fibers had the lowest storage modulus and the highest loss factor (Figure 7). Adding carbon nanotubes to the fiber reinforced composites further increased the storage modulus with increasing nanotube content, which indicates that the nanotubes dispersed well in the composite and connected strongly to the matrix.

The peaks of the loss factor curves decreased with increasing nanotube content and shifted to higher temperatures, which means that the storage modulus drop at the glass transition temperature was significantly lower compared to either the PA6 reinforced with only carbon fibers or the pure PA6 (Figure 7.b). This is because the mobile amorphous fractions represented a smaller volume fraction and were also less mobile in the nanocomposites than in the pure PA6. The size of the second peak, which depends the modulus drop caused by the motion of the segments in the rigid amorphous phase, also increased with higher nanotube content. This is caused by the higher volume fraction of the rigid amorphous parts. As a result, the previously mentioned two-layer interphase that formed an immobilized polymer layer around the reinforcing materials had an additional reinforcing effect in addition to the carbon fibers and the carbon nanotubes.

a)   b)
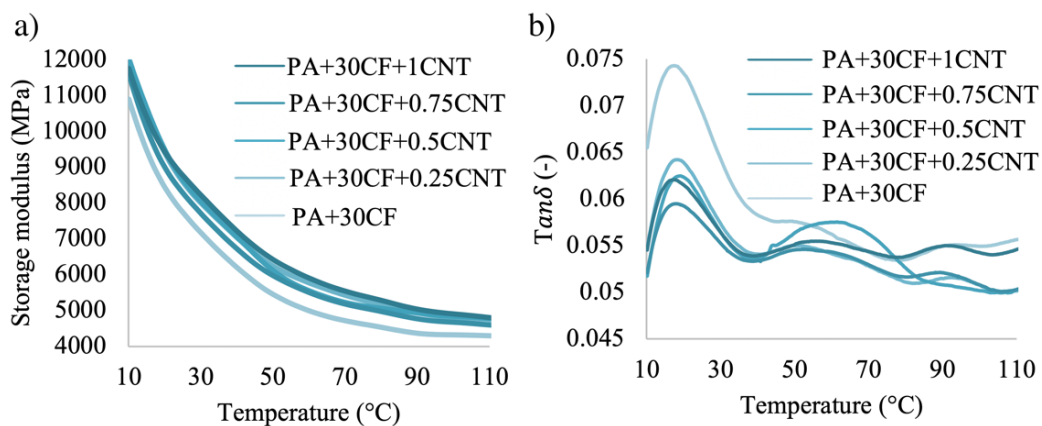
Figure 7 a) storage modulus and b) loss factor curves of the composites containing carbon fiber

4. Conclusion

In this project, we investigated the microstructure and dynamic mechanical properties of carbon fiber and carbon nanotube reinforced nano- and hybrid composites. The DSC tests showed that in the nanocomposites, a two-layer interphase was formed around the CNT bundles, where the inner layer is a crystalline phase and the outer layer is a rigid amorphous phase. However, the volume fraction of the crystalline and the rigid amorphous fractions decreased with the presence of carbon nanotubes compared to the pure PA6. In the hybrid composites, both the carbon fibers and the carbon nanotubes had a crystal nucleating effect; similarly to the nanocomposites, a two-layer interphase was formed with a trans-crystalline inner, and a rigid amorphous outer layer. In the hybrid composites, the nano- and the micro-sized reinforcement had a synergistic effect as the volume fraction of both the crystalline and the rigid amorphous fractions increased compared to the pure or the PA6 reinforced with only carbon fibers.

The dynamic mechanical tests showed that in the nanocomposites, the lower volume fraction of the crystalline interphase and the rigid amorphous interphase around the carbon nanotubes slightly decreased the loss factor peaks and the storage modulus. In the hybrid composites, where the carbon fibers helped disperse the carbon nanotubes uniformly, the storage modulus drop at the glass transition temperature was significantly lower compared to that of either the PA6 reinforced with only carbon fibers or the pure PA6. The two-layer interphase around the reinforcing materials not only helped transfer the stress from the matrix to the reinforcement but acted as an additional reinforcing component as well.

References

[1]　Eitan A et al 2006 *Compos. Sci. Technol.* **66** 1162-73
[2]　Gojny F H et al 2005 *Compos. Sci. Technol.* **65** 2300-13
[3]　Odegard G M et al 2005 *Polymer.* **46** 553-62
[4]　Ansari R and Hassanzadeh-Aghdam M K 2016 *Int. J. Mech. Sci.* **115-116** 45-55
[5]　Bershtein et al 2019 *Express Polym. Lett.* **13** 656-672
[6]　Patel R K et al 2008 *Mech. Res. Comm.* **35** 115-25
[7]　Prusty R K et al 2017 *Adv. Colloid Interfac.* **240** 77-106
[8]　Lipatov Y S 1977 *Physical Chemistry.* (Berlin, Heidelberg: Springer Berlin Heidelberg)
[9]　Chen H and Cebe P 2007 *J. Therm. Anal. Calorim.* **89** 417-25
[10]　Szakács J et al (2019) *J. Therm. Anal. Calorim.* **137** 43–53
[11]　Wang X D et al (2008) *Polym. J.* **40** 450-454
[12]　Cruz et al 2019 *Express Polym. Lett.* **9** 825-834
[13]　Hajba S and Tábi T 2019 *Period. Polytech. Mech. Eng.* **63** 270-277
[14]　Logakis et al 2009 *J. Polym. Sci. Pol. Phys.* **47** 764-774
[15]　Brosse et al 2008 *Polymer.* **49** 4680-4686